J. Appl. Comput. Mech., 12(1) (2026) 202-211
DOI: 10.22055/jacm.2025.48309.5135

ISSN: 2383-4536
jacm.scu.ac.ir

Shahid Chamran University of Ahvaz

Journal of Applied and Computational Mechanics

Research Paper

Analysis of the Effects of Time Periods and Fractal Patterns on Heat Flow in Porous Materials

A.M. Al Khulayf[1], A.N. Abdalla[2], F.A. Alshehri[3], A. Alasmari[4], A. Ismail[5], A.A. Kilany[6]

[1] Department of Mathematics, College of Science and Humanities in Alkharj, Prince Sattam Bin Abdulaziz University, Alkharj 11942, Saudi Arabia

[2] Department of Mathematics, Faculty of Science, Sohag University, 82425 Sohag, Egypt

[3] Department of Mathematics, College of Sciences, University of Bisha, P.O Box 8154, 67398-5644 Alnamas, Saudi Arabia

[4] Department of Physics, College of Science, University of Bisha, Bisha 61922, Saudi Arabia

[5] Department of Physics, Al-Azhar University, 71524 Asyut, Egypt

[6] Ministry of Higher Education, Higher Institute of Management Sciences, Beni Suef, Egypt

Received March 15 2025; Revised May 05 2025; Accepted for publication May 09 2025.
Corresponding author: A.N. Abdalla (aboelnourabdalla@yahoo.com)

Abstract. The proposed mathematical model applies non-integer derivative orders to study how porosity influences a generalized thermoelastic medium while utilizing improved multi-phase delays framework. The system consists of a porous homogenous isotropic domain where the volume percent shows two-dimensional variations. The modified couple stress theory enables transformation of controlling differential equations into ordinary differential equations. Declining to the normal mode approach allows analysis of these equations' mathematical solutions. The calculation of precise solutions for displacement, temperature change, shear and perpendicular loads and volume fraction parameter depends on harmonic wave analysis. The research outcomes present graphical illustrations which present the influence of complex derivative orders together with material porosity levels. The paper demonstrates how models that use fractal differentiation differ from standard models through comparison studies. The research findings enhance thermoelastic behavior understanding in porous media while facilitating the creation of improved performance materials. The study provides significant ramifications for materials science and offers solutions to multi-physics problems as well as enables the development of high-precision industrial technologies.

Keywords: Generalized thermoelasticity; Non-integer derivative order; Refined multi-phase lags model; Porous media; Harmonic wave analysis.

1. Introduction

As there have been tremendous developments in the theories of partial thermoelasticity and theories of porous materials [1-5] in recent times, modern studies have been able to discover and understand the mechanical, thermal and non-local effects coupled in complex structures. Researches developed an extended method for classical elastic modeling of complicated material behaviors including anomalous diffusion by implementing partial calculus with spatial separation of kinematic variables and small pore consideration. These analytic approaches become operational under severe environmental factors to study complex mechanical systems which find practical usage in geology and biomechanics and biomedical systems. Thermoelasticity achieved significant theoretical advancements by using generalized and modified theories to overcome non-classical phenomena according to research works in [6-8]. Modern thermoelastic theories gained their principles through these seminal discoveries which enabled the explanation of wave motion and energy transfer processes and relaxation in advanced systems and materials.

Fractional calculus has lately enhanced the modeling of thermoelastic and heat conduction phenomena. A basic construction of fractional derivatives, which can be widely used in many fields such as science and engineering, was developed by Podlubny [9]. Memory effects and non-local features in fractional-order thermoelasticity were added, which were also proposed by Sherif et al. [10]. Ezzat [11] extended this approach to magneto-thermoelasticity with thermoelectric properties, where studies were adapted in multiphysics systems. Furthermore, Zakaria et al. [12] used fractional thermoelasticity on semiconductors, whilst Zenkour and Abouelregal [13] and Ma et al. [14] investigated heat conduction and electro-magneto-thermoelastic issues, respectively. The work conducted by Ma et al. [14] builds on important developments in partial thermoelasticity, including studies on the coupling of thermoelasticity with electromagnetism. While Youssef [15, 16] addressed the topic of generalized thermoelasticity with partial strain considering partial thermoelastic effects in complex geometries and nanostructures. Also, there are strong foundations for investigating the interaction between thermal, mechanical and electromagnetic phenomena in advanced materials [17-21].

Published online: May 15 2025

Abbas et al. [22, 23] have made significant contributions to thermoelasticity and photothermal theory. Their research encompasses hyperbolic two-temperature effects in semiconductors, generalized thermoelasticity in advanced materials and microstructures [24-26], wave propagation in complex solids [27], and thermal diffusion in thermoelastic media [28]. These studies provide essential frameworks for understanding coupled thermal-mechanical-optical behaviors in various materials. Abouelregal and his distinguished research group [29-31] have made significant contributions to advanced thermoelastic studies with a modified fractal model with multiple relaxation times for spherical cavities under harmonic heating. Furthermore, they studied the propagation of thermal waves in non-local media with moving heat sources. They also proposed a temporally non-local thermoelastic theory for polar microscopic viscoelastic media under laser excitation. Osman et al. [32, 33] have studied fractional heat transfer in fiber reinforced materials, three-phase delay effects in thermoelastic media [34, 35], memory-based derivatives and laser heating [36], magnetic field effects [37], and laser pulse effects in porous media [38].

The main purpose of this research involves creating a mathematical model to evaluate porous medium generalized thermoelasticity based on Lord–Shulman (L-S) and dual-phase-lag (RPL) theories. The model exists under a new analytical framework that uses non-integer derivative order analysis to present an innovative view on fractional calculus applications. This novel operational approach demonstrates ways to improve knowledge of heat transfer techniques by considering the detailed interrelationships between mechanical and thermal properties of materials during the analysis of complex and microstructure components. The newly proposed fractional thermos-elasticity framework proves best suited for studying heat conduction within nanometer-scale bodies including nanowires and nanotubes. The research investigates the impact that thermal relaxation times together with porosity have on physical variable distributions of stresses, displacements, temperature and volume fraction fields.

2. Mathematical Preliminaries

Fractional calculus functions as a generalized version of traditional calculus which expands integration and differentiation to fractional-order calculations apart from standard integer values. Fractional calculus provides scientists with an effective tool to recognize memory patterns and family traits throughout various technical and physical systems. The anomalous systems that include electrical circuits and viscoelastic materials and diffusion processes use fractional derivatives to solve FDEs. The concepts and critical attributes of fractional differential equation calculus receive detailed description in subsequent sections to support better comprehension (refer to [29–34] for comprehensive details).

2.1. Definition

The Riemann-Liouville integral is driven by the Cauchy formulation for successive integration. For a f continuous on the period [0, x], the Cauchy formula for n-fold repeating integration indicates:

$$J^{\alpha} f(x)=\frac{1}{(n-1)}\int_0^x (x-t)^{\alpha-1} f(t)dt, x>0, \alpha>0 \tag{1}$$

Now, the fractional integral operator of Riemann–Liouville of order $\alpha \geq 0$, of a function $f \in C\mu, \mu \leq -1$, may be written as:

$$\begin{gathered} J^{\alpha} f(x)=\frac{1}{\Gamma(\alpha)}\int_0^x (x-t)^{\alpha-1} f(t)dt, x>0, \alpha>0 \\ J^0 f(x)=f(t) \end{gathered} \tag{2}$$

2.2. Properties of the operator J^{α}

For $f \in C\mu, \mu \leq -1$, $\alpha, \beta > 0$, and $\gamma \leq -1$, one has:

$$J^{\alpha} J^{\beta} f(x)=J^{\alpha+\beta} f(x) \tag{3a}$$

$$J^{\alpha} J^{\beta} f(x)=J^{\beta} J^{\alpha} f(x) \tag{3b}$$

$$J^{\alpha} x^{\gamma}=\frac{\Gamma(\gamma+1)}{\Gamma(\gamma+\alpha+1)} x^{\alpha+\gamma} \tag{3c}$$

2.3. Definition

According to the Caputo method, the fractional derivative of $f(x)$ is given by:

$$D^{\alpha} f(x)=J^{m-\alpha} D^m f(x)=\frac{1}{\Gamma(m-\alpha)}\int_0^x (x-t)^{m-\alpha-1} f^{(m)}(t)dt, \quad m-1<\alpha<m, m\in N, x>0 \tag{4}$$

2.4. Definition

The smallest integer that surpasses α, the Caputo fractional derivatives of order $\alpha > 0$ is known is seen as:

$$D^{\alpha} f(x,t)=\frac{\partial^{\alpha} f(x,t)}{\partial t^{\alpha}}=\begin{Bmatrix} \dfrac{1}{\Gamma(m-\alpha)}\displaystyle\int_0^t (t-\tau)^{\varepsilon-1}\frac{\partial^{\alpha} f(x,t)}{\partial t^{\alpha}} d\tau, m-1<\alpha\leq m \\ \dfrac{\partial^{\alpha} f(x,t)}{\partial t^{\alpha}}, \alpha=m\in N \end{Bmatrix} \tag{5}$$

2.5. Properties

The operator for D^{α} of the Caputo fractional derivatives of order $\alpha > 0$, will take the following form:

$$D^{\alpha} x^{\gamma}=\frac{\Gamma(\gamma+1)}{\Gamma(\gamma-\alpha+1)} x^{\gamma-\alpha}, \quad D^{\alpha} e^t=t^{-\alpha}\sum_{n=0}^{\infty}\frac{t^n}{\Gamma(n-\alpha+1)} \tag{6}$$

3. Basic Equations

We consider a plane strain state confined to the *xy*-plane. The three principal variables in this context are:

i. Displacement field, $u_i(x,y,t)$: This represents the elastic waves propagating through the material. The vector u_i (where $i=1,2$) corresponds to the displacement components along the x- and y-axes, respectively.

ii. Temperature field, $T(x,y,t)$: This describes the thermal waves and their distribution across the medium, accounting for thermal conduction and temperature gradients.

iii. Volume fraction field, $\phi_i(x,y,t)$: This represents the porosity-related variations within the material. Also, it is essential to realizing how the fluid and solid phases interact in porous thermoelastic media.

In this model, we employ the standard tensor notation alongside Einstein's summation convention for clarity and compactness. All previously introduced symbols, operators, and notations follow the definitions provided in Nomenclature.

The coupled equations for motion, heat conduction, and volume fraction are formulated within generalized thermoelasticity, incorporating fractional of Riemann-Liouville derivative of order $\alpha > 0$, to capture memory effects and influenced by porosity and refined multi-phase lag (MPL) parameters.

(1) In generalized thermoelasticity with fraction field, the equation of motion for an isotropic homogeneous body may be expressed as follows:

$$\mu\nabla_\alpha^2 u_i + (\lambda+\mu)\nabla_\alpha e - \gamma\nabla_\alpha T + b_v\nabla_\alpha\phi_v = \rho D_t^{\alpha\alpha}u_i \tag{7}$$

(2) The generalized thermoelasticity refinement multi-phase lag system with fraction field is the basis for the heat conduction equation, which may be represented as follows:

$$K\left(1+\sum_{r=1}^{M}\frac{\tau_\theta^r}{r}D_{t^r}^{\alpha^r}\right)\nabla_\alpha^2 T = \left(\Im + \tau_o D_t^\alpha + \sum_{r=1}^{M}\frac{\tau_q^{r+1}}{(r+1)!}D_{t^{r+1}}^{\alpha^{r+1}}\right)\times[\rho c_e D_t^\alpha T + T_o\gamma D_t^\alpha e + mT_o D_t^\alpha\phi_v] \tag{8}$$

(3) The volume fraction field equation takes the form:

$$\alpha\phi_{v_{,ii}} - b_v u_{i,i} - \zeta\phi_v - \omega_v\dot{\phi}_v + mT = \rho\chi\ddot{\phi}_v \tag{9}$$

(4) The constitutive relations are considered as:

$$\sigma_{ij} = 2\mu\varepsilon_{ij} + [\lambda e - \gamma T + b_v\phi_v]\delta_{ij} \tag{10}$$

$$\varepsilon_{ij} = \frac{1}{2}(u_{i,j}+u_{j,i}), e = u_{i,i}, i,j = 1,2,3 \tag{11}$$

4. Formulation of the Problem

Using the specified nondimensional variables, the equations are simplified and normalized to facilitate the analysis. By using the following nondimensional variables to the above equations:

$$\begin{gathered}(x',y',u',v') = \frac{1}{C_T t^{*\alpha}}(x,y,u,v), (t',\tau_0',\tau_q',\tau_\theta') = \frac{1}{t^{*\alpha}}(t^\alpha,\tau_0,\tau_q,\tau_\theta), (T',\phi_v') = \frac{1}{(\lambda+2\mu)}(\gamma T,\chi\phi_v),\\ \sigma_{ij}' = \frac{1}{\mu}\sigma_{ij}, C_T^2 = \frac{\lambda+2\mu}{\rho}, t^{*\alpha} = \frac{K}{\rho c_e C_T^2},\end{gathered} \tag{12}$$

The displacement potentials $\Phi(x,y,t)$ and $\Psi(x,y,t)$ are introduced to express the displacement components $u_i(x,y,t)$ in terms of scalar and vector potentials, respectively. This is represented as:

$$\vec{u} = \vec{\nabla}_\alpha\Phi + \vec{\nabla}_\alpha\times\Psi \tag{13}$$

where Φ accounts for longitudinal displacements and Ψ represents shear wave components. This approach significantly simplifies the governing equations.

Substituting the expressions from Eqs. (1)-(11) into Eqs. (12)-(13), we derive the equations governing the scalar potential Φ and the vector potential Ψ. These equations encapsulate the dynamics of the thermo-elastic and porosity effects, considering the influence of fractional derivatives. Therefore, we have:

4.1. Equation for scalar potential Φ

This equation combines the effects of porosity, temperature field, and fractional derivative terms. By using Eqs. (1)-(14), in Eqs.(12)-(13), we obtain:

$$[\nabla_\alpha^2 - D_t^{\alpha\alpha}]\Phi - T - N + \hat{b}\phi_v = 0 \tag{14}$$

$$[\nabla_\alpha^2 - \beta^2 D_t^{\alpha\alpha}]\Psi = 0 \tag{15}$$

$$K\left(1+\sum_{r=1}^{M}\frac{\tau_\theta^r}{r}D_{t^r}^{\alpha^r}\right)\nabla_\alpha^2 T = \left(\Im + \tau_o D_t^\alpha + \sum_{r=1}^{M}\frac{\tau_q^{r+1}}{(r+1)!}D_{t^{r+1}}^{\alpha^{r+1}}\right)\times[D_t^\alpha T + \varepsilon_1\nabla_\alpha^2\Phi + \varepsilon_2 D_t^\alpha\phi_v] \tag{16}$$

$$[\nabla_\alpha^2 - S_2 - S_3 D_t^\alpha - S_5 D_t^{\alpha\alpha}]\phi_v - S_1\nabla_\alpha^2\Phi + S_4 T = 0 \tag{17}$$

4.2. Stress components

The stress components can be written as follows:

$$\sigma_{xx} = \beta^2 D_x^\alpha u + (\beta^2 - 2) D_y^\alpha v - \beta^2 T + \beta^2 \hat{b}\phi_v \tag{18}$$

$$\sigma_{yy} = (\beta^2 - 2) D_x^\alpha u + \beta^2 D_y^\alpha v - \beta^2 T + \beta^2 \hat{b}\phi_v \tag{19}$$

$$\sigma_{zz} = (\beta^2 - 2)\nabla_\alpha^2 \varPhi - \beta^2 T + \beta^2 \hat{b}\phi_v \tag{20}$$

$$\sigma_{xy} = D_y^\alpha u + D_x^\alpha v \sigma_{xz} = \sigma_{yz} = 0 \tag{21}$$

where, we have used:

$$\varepsilon_1 = \frac{\gamma^2 T_0 t^{*\alpha}}{K\rho}, \varepsilon_2 = \frac{mT_0\gamma}{\rho c_e \chi}, S_1 = \frac{b_v t^{*\alpha 2}\chi}{\alpha_1 \rho}, S_2 = \frac{\zeta C_T^2 t^{*\alpha 2}}{\alpha_1}, S_3 = \frac{\omega_v C_T^2 t^{*\alpha}}{\alpha_1}, S_4 = \frac{mC_T^2 t^{*2}\chi}{\alpha_1 \gamma}, S_5 = \frac{\rho C_T^2 \chi}{\alpha_1}, \quad \beta^2 = \frac{\lambda + 2\mu}{\mu}, \hat{b} = \frac{b_v}{\chi},$$

5. Harmonic Wave Technique

The harmonic wave technique was used to solve the governing equations (14) through (17) by converting them from partial differential equations to ordinary differential equations. As a result, the harmonic wave process can be stated as follows [32]:

$$[\varPhi, \varPsi, T, \phi_v, \sigma_{ij}](x, y, t) = [\varPhi^*, \varPsi^*, T^*, {\phi_v}^*, \sigma_{ij}^*](x)\, exp(\omega t^\alpha + iby^\alpha) \tag{22}$$

Using Eq. (22), Eqs. (14)-(17) become as:

$$(D_x^{\alpha\alpha} - A_1)\varPhi^* - T^* + \hat{b}\phi_v^* = 0 \tag{23}$$

$$(D_x^{\alpha\alpha} - A_2)\varPsi^* = 0 \tag{24}$$

$$-A_3(D_x^{\alpha\alpha} - b^2)\varPhi^* - (D_x^{\alpha\alpha} - \varGamma_2)T^* - A_4\phi_v^* = 0 \tag{25}$$

$$-S_1(D_x^{\alpha\alpha} - b^2)\varPhi^* + (D_x^{\alpha\alpha} - A_5)\phi_v^* + S_4 T^* = 0 \tag{26}$$

where,

$$A_1 = \alpha^2 b^2 + \alpha^2\omega^2, A_2 = \alpha^2 b^2 + \alpha^2\beta^2\omega^2, A_3 = \varGamma_1\varepsilon_1, A_4 = \varGamma_1\varepsilon_2, \varGamma_2 = \alpha^2 b^2 + \varGamma_1, A_5 = \alpha^2 b^2 + S_2 + \alpha S_3\omega + \alpha^2 S_5\omega^2,$$
$$\varGamma_\theta = \left(1 + \sum_{r=1}^{M} \frac{\tau_\theta^r}{r}\alpha^r\omega^r\right), \varGamma_q = \left(\Im + \tau_o\alpha\omega + \sum_{r=1}^{M}\frac{\tau_q^{r+1}}{r+1}\alpha^{r+1}\omega^{r+1}\right), \varGamma_1 = \frac{\alpha\omega\varGamma_q}{\varGamma_\theta}$$

Eliminating $\varPhi^*(x), T^*(x), \phi_V^*(x)$ between Eqs. (18), (21), and (24) the following six-order ordinary differential equation as:

$$\alpha^6 D^6 - A\alpha^4 D^4 + B\alpha^2 D^2 - C = 0 \tag{27}$$

where,

$$A = -\hat{b}S_1 + A_1 + A_3 + A_5 + \varGamma_2, B = A_4(S_4 - S_1) + A_3\alpha^2 b^2 + A_5(A_1 + A_3) + \varGamma_2(A_1 + A_5) - A_3\hat{b}S_4 - \hat{b}S_1(\varGamma_2 + \alpha^2 b^2)$$
$$C = -(A_4\alpha^2 b^2 S_1 - A_1 A_4 S_4 - A_3 A_5 \alpha^2 b^2 - A_1 A_5 \varGamma_2 - A_3\alpha^2 b^2\hat{b}S_4 + \alpha^2 b^2\hat{b}S_1\varGamma_2)$$

Equation (23) can be factored as:

$$\alpha^6(D_\alpha^2 - k_1^2)(D_\alpha^2 - k_2^2)(D_\alpha^2 - k_3^2)\{\varPhi^*, T^*, {\phi_v}^*\} = 0 \tag{28}$$

where $k_j^2, j = 1{,}2{,}3$ are the roots of the characteristic equation of Eq. (28). The solution of Eq. (28), bounded as $x \to \infty$, is:

$$\varPhi^* = \sum_{n=1}^{3} M_n\, e^{-k_n x^\alpha} \tag{29}$$

$$T^* = \sum_{n=1}^{3} H_{1n} M_n\, e^{-k_n x^\alpha} \tag{30}$$

$${\phi_v}^* = \sum_{n=1}^{3} H_{2n} M_n\, e^{-k_n x^\alpha} \tag{31}$$

The solution of Eq. (24) may be represented as:

$$\varPsi^* = M_4 e^{-\sqrt{A_2}x^\alpha} \tag{32}$$

The following form may be used to obtain the displacement components:

$$u = -\sum_{n=1}^{3} \alpha k_n M_n\, e^{-k_n x^\alpha + \omega t^\alpha + iby^\alpha} + i\alpha b M_4 e^{-\sqrt{A_2}x^\alpha + \omega t^\alpha + iby^\alpha} \tag{33}$$

$$v = \sum_{n=1}^{3} i\alpha b M_n\, e^{-k_n x^\alpha + \omega t^\alpha + iby^\alpha} + \sqrt{A_2} M_4 e^{-\sqrt{A_2}x^\alpha + \omega t^\alpha + iby^\alpha} \tag{34}$$

Using above equations, we obtain:

$$\sigma_{xx} = \sum_{n=1}^{3} H_{3n} M_n \, e^{-k_n x^\alpha + \omega t^\alpha + iby^\alpha} - 2i\alpha b\sqrt{A_2} M_4 e^{-\sqrt{A_2}x^\alpha + \omega t^\alpha + iby^\alpha} \tag{35}$$

$$\sigma_{xy} = -\sum_{n=1}^{3} H_{4n} M_n \, e^{-k_n x^\alpha + \omega t^\alpha + iby^\alpha} - (\alpha^2 b^2 + A_2) M_4 e^{-\sqrt{A_2}x^\alpha + \omega t^\alpha + iby^\alpha} \tag{36}$$

where,

$$\Lambda_{1n} = \alpha^2 k_n^2 - A_1, \Lambda_{2n} = \alpha^2 k_n^2 - \Gamma_2, \Lambda_{3n} = \alpha^2 k_n^2 - \alpha^2 b^2, H_{1n} = \frac{A_4 \Lambda_{1n} - A_3 \hat{b} \Lambda_{3n}}{A_4 + \hat{b}\Lambda_{2n}}, H_{2n} = \frac{H_{1n} + \Lambda_{1n}}{\hat{b}},$$

$$H_{3n} = \beta^2 \left(\alpha^2 k_n^2 - \alpha^2 b^2 - H_{1n} + \hat{b} H_{2n}\right) + 2\alpha^2 b^2, H_{4n} = 2i\alpha^2 b k_n$$

6. Boundary Conditions

To determine the unknown parameters, we can use boundary conditions on $x = 0$:

$$\sigma_{xx} = -f_1^* e^{\omega t^\alpha + iby^\alpha}, \sigma_{xy} = 0, D_x^\alpha T = 0, D_x^\alpha \phi_v = 0 \tag{37}$$

Using the boundary conditions (37) at the surface yields a system of four equations. Upon performing the inverse matrix approach, one may get:

$$\begin{pmatrix} M_1 \\ M_2 \\ M_3 \\ M_4 \end{pmatrix} = \begin{pmatrix} H_{31} & H_{32} & H_{33} & -2i\alpha b\sqrt{A_2} \\ H_{41} & H_{42} & H_{43} & (\alpha^2 b^2 + A_2) \\ \alpha k_1 H_{11} & \alpha k_1 H_{12} & \alpha k_1 H_{13} & 0 \\ \alpha k_1 H_{21} & \alpha k_1 H_{22} & \alpha k_1 H_{23} & 0 \end{pmatrix}^{-1} \begin{pmatrix} -f_1^* \\ 0 \\ 0 \\ 0 \end{pmatrix} \tag{38}$$

7. Numerical Results and Discussion

The Magnesium (Mg) medium is used for numerical estimates. The specifications for (Mg) as a porous medium are shown in [21]:

$$\begin{gathered} \lambda = 2.17 \times 10^{10} Nm^{-2}, \mu = 3.278 \times 10^{10} Nm^{-2}, \rho = 1740 \mathrm{kg} m^{-3}, K = 1.7 \mathrm{wm}^{-1} k^{-1}, c_e = 1040 J.\mathrm{kg}^{-1}.\, K^{-1}, \\ b = 1.5, y = 0.05, i = \sqrt{-1}, f_1^* = 1, \alpha_t = 1.98 \times 10^{-6} k^{-1}, T_0 = 298K, \zeta = 0.04, \omega_0 = 1, \omega = \omega_0 + i\zeta \end{gathered} \tag{39}$$

For voids parameters, it is considered:

$$\begin{gathered} b_v = 1.13840 \times 10^{10} Nm^{-2}, \omega_v = 0.0787 \times 10^{-3} Nm^{-2} s^{-1}, \chi = 1.753 \times 10^{-15} m^2, \alpha_1 = 3.688 \times 10^{-5} N, \\ m = 2 \times 10^6 Nm^{-2}.\, K^{-1}, \zeta = 1.475 \times 10^{10} Nm^{-2}. \end{gathered} \tag{40}$$

Figure 1 shows a schematic of porous medium with voids. It depicts a rectangle domain depicting the porous media (magnesium), with green oval shapes indicating voids scattered inside the solid matrix, which is critical to the investigation.

In summary, the study looks at the effect of porosity on a generalized thermoelastic media in a multi-phase delay framework with non-integer derivative orders. This has major implications for understanding and designing materials and systems in various engineering disciplines as: (1) Geothermal energy and oil/gas recovery, (2) Porous material design for thermal insulation and damping, (3) Nuclear waste disposal, (4) Biomechanics and tissue engineering and (5) Advanced composite materials.

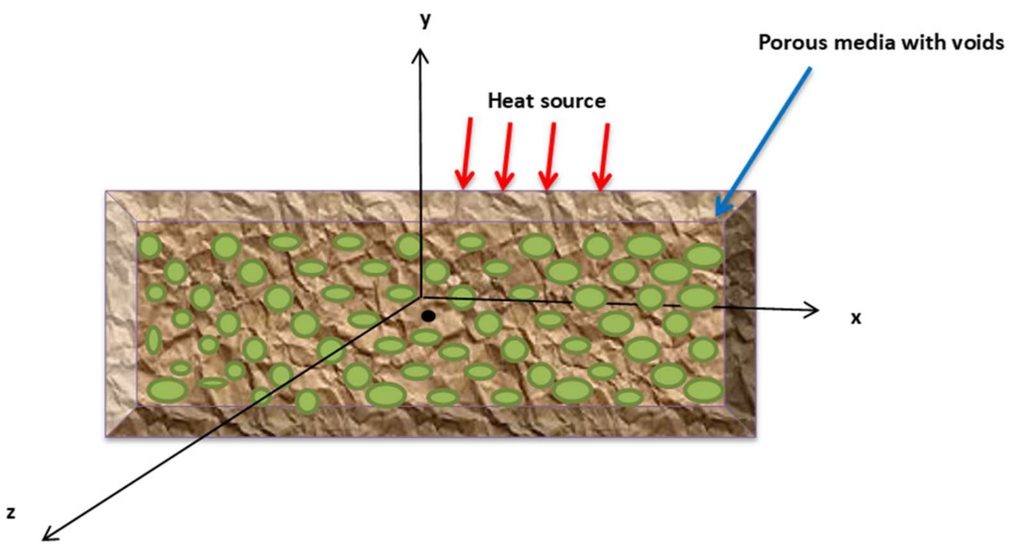

Fig. 1. Geometry of the problem.

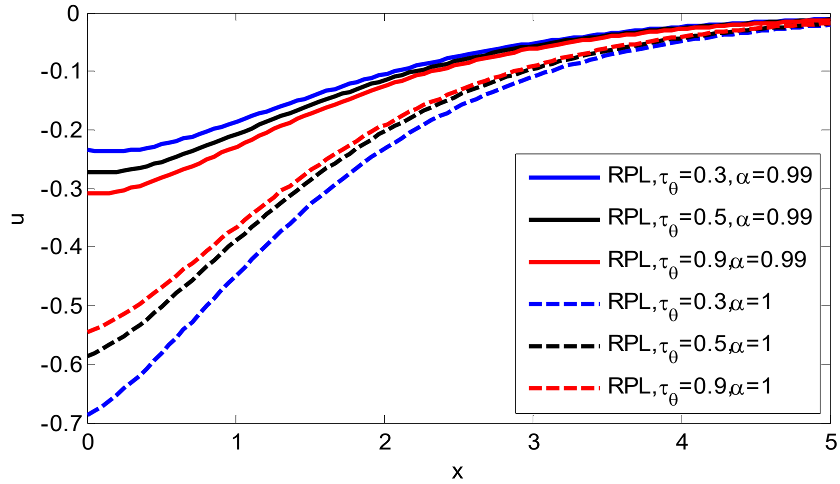

Fig. 2. The fractional solution for horizontal displacement distribution u with change of relaxation time with and without fractional parameters (α = 0.99, 1).

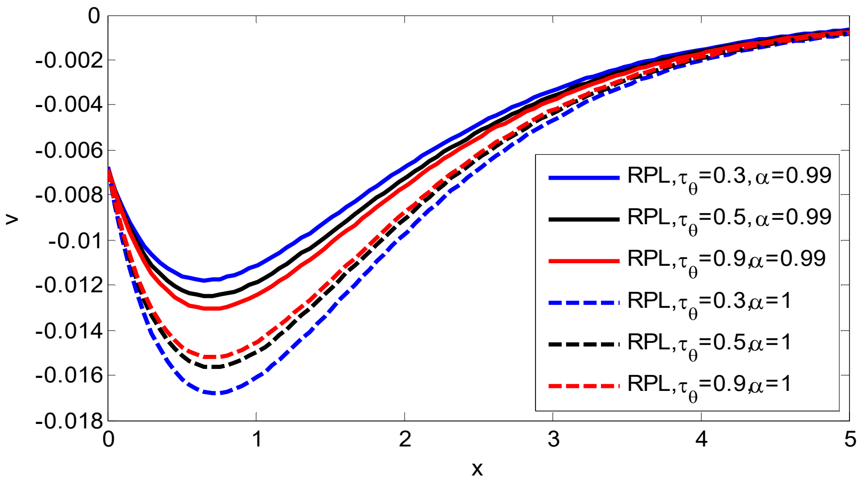

Fig. 3. The fractional solution for vertical displacement distribution v with change of relaxation time with and without fractional parameters (α = 0.99, 1).

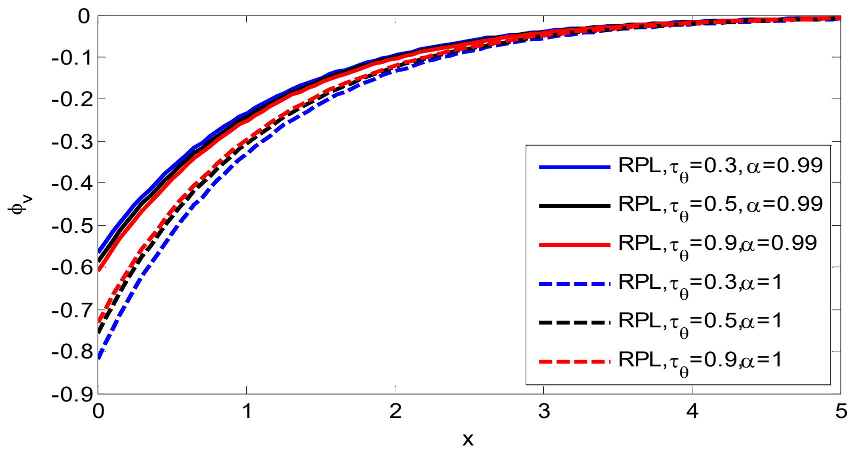

Fig. 4. The fractional solution for the variations of concentration ϕ_v with change of relaxation time with and without fractional parameters (α = 0.99, 1).

In all presented results, we used the horizontal axis represents a spatial dimension x as independent variable, while the vertical axis depicts the others dependent variables such as the horizontal displacement distribution u, the vertical displacement distribution v, the variations of concentration ϕ_v, the variations of the stresses σ_{xx} and σ_{yy} and the variations of temperature T of the medium. The core purpose is to visualize how dependent variables change under different conditions, specifically varying the relaxation time τ_θ and the order of differentiation (α = 0.99, 1, i.e., fractional or standard). In general, we used the well-known program MATLAB to make programs and calculate this research.

We will now summarize in the following section the most important comments, explanations, notes and important results represented in the graphs and numbered from 2 to 7 as follows:

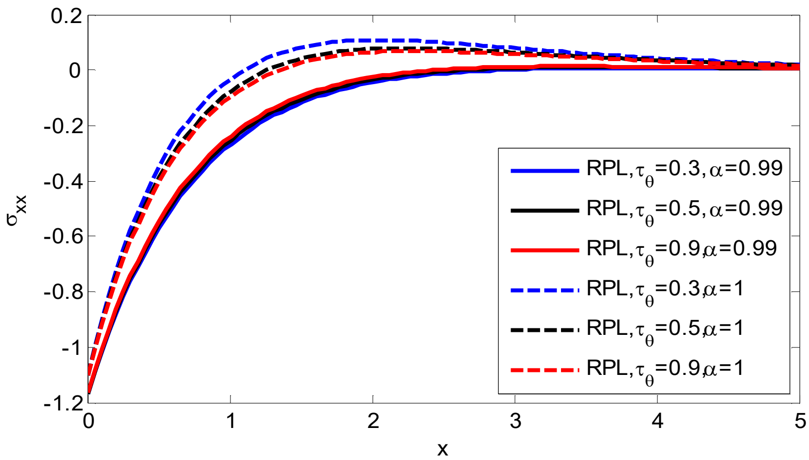

Fig. 5. The fractional solution for the variations of stress σ_{xx} with change of relaxation time with and without fractional parameters (α = 0.99, 1).

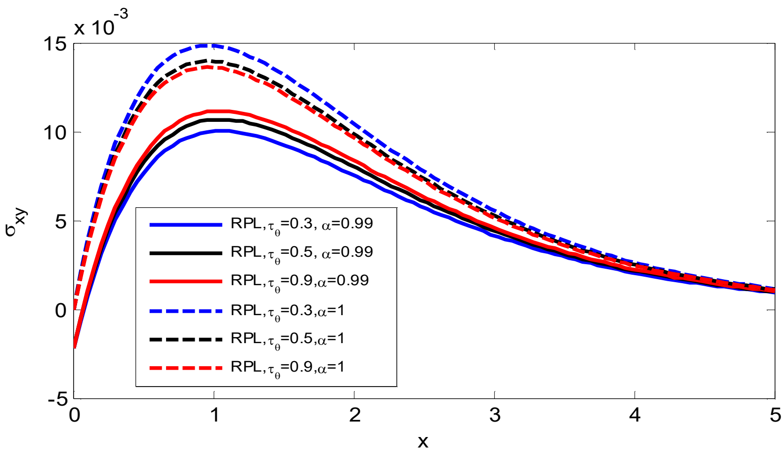

Fig. 6. The fractional solution for the variations of stress σ_{xy} with change of relaxation time with and without fractional parameters (α = 0.99, 1).

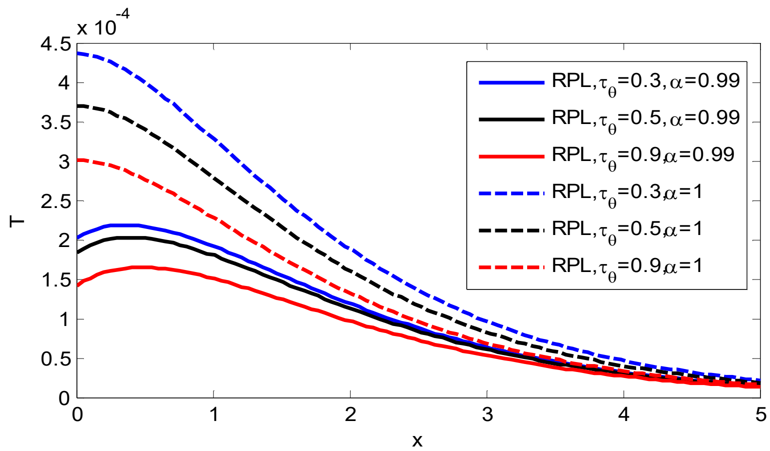

Fig. 7. The fractional solution for the variations of temperature T with change of relaxation time with and without fractional parameters (α = 0.99, 1).

Figure 2 plots the horizontal displacement (u) inside a porous medium of (Mg) where relaxation time (τ_θ) and fractional differentiation (α) affect the system results. Standard differentiation appears as solid lines for α = 1 with fractional differentiation shown as dashed lines for α = 0.99. The relaxation times (τ_θ = 0.3, 0.5, 0.9) correspond to different color indicators. Since some basic remarks are included in the next part:

- According to the presented data, the magnitude of displacement u decreases as the horizontal variable increases.
- During the transient process the rising values of relaxation time (τ_θ) correlate with stronger displacement intensity.
- Fractional differentiation alters the shape of displacement variation resulting in improved mathematical models to analyze stimuli response in media.
- The results show a particular mode of deformation occurs within the medium.
- It is noted that the displacement increases with relaxation time (τ_θ) until the implementation of fractional differentiation yet decreases with relaxation time (τ_θ) after the introduction of fractional differentiation in the model structure.

The main purpose of the above figure is to see how the displacement changes under different relaxation times and with or without fractional differentiation

Figure 3 shows how (Mg) porous medium displacement (v) changes vertically across the spatial dimensions (x) under relaxation time (τ_θ) and fractional differentiation parameter (α) influence. This research contains a comparative study between two (α) values where α = 1 depicts no fractional differentiation while α = 0.99 indicates its application. The vertical displacement magnitude (v) rises with increasing horizontal distance (x) under conditions where α takes the value of 1. The system reacts differently because of fractional differentiation when α = 0.99 as the magnitude of (v) demonstrates a reduction with increasing x distance.

The (RPL, τ_θ) theory controls displacement profile characteristics through different conditions that include (τ_θ = 0.3, 0.6, 0.9). The displacement distribution curves shift based on changes in the value of τ_θ for both α settings because the initial state plays a major role in distributing displacement disorder. The negative sign of (v) represents motion which seems to occur in a downward direction. Our model results demonstrate why adopting fractional differentiation effects through α = 0.99 requires study when compared to the standard value of α = 1 when representing porous media systems. The displacement characteristics diverge between fractional differentiation models because these techniques bring non-local as well as memory effects into the system

Figure 4 shows the change in concentration ϕ_v inside a porous (Mg) medium as a function of the horizontal axis x in an attempt to know the effect of changing the relaxation time and fractional differentiation. In other words, it is a visualization of how the concentration of the porous medium changes under different conditions.

- Important points to note

- Different colored lines in the graph demonstrate varying values of Relaxation Time Parameter (RPL, τ_θ). The curves experience movement according to changes in (RPL, τ_θ) values. The relaxation time controls how the concentration evolves throughout time. Systems with longer (RPL, τ_θ) values create different concentration patterns because the relaxation process until reaching equilibrium takes prolonged time periods.
- The figure displays the results from two differentiation techniques where standard differentiation appears as solid lines while fractional differentiation shows its effects through dashed lines. The value of fractional differentiation parameter α = 1 demonstrates classic differentiation and the α = 0.99 displays its advanced fractional properties.
- Fractional differentiation produces small yet perceptible differences between solid and dashed patterns which indicates fractional calculus better describes how the concentration behaves in this case.
- Finally, Fig. 3 illustrates how relaxation time works together with fractional differentiation to shape the concentration levels. The set of curves demonstrates distinct (RPL, τ_θ) values and α levels which display their combined relationship.
- The behavior of σ_{xx} and σ_{xy} stresses within Magnesium porous medium under relaxation time effects and fractional differentiation appears in Figs. 5 and 6.

Figure 5 shows σ_{xx} variations. The x-axis represents the horizontal axis whereas the y-axis shows the stress σ_{xx}. The analysis contains two sets of stress measurements that demonstrate fractional differentiation through α = 0.99 (dashed lines) with α = 1 (solid lines) displaying the other scenario. The relaxation time parameter (RPL, τ_θ) possesses different values between 0.3, 0.5, and 0.9 for the multiple lines presented. The data shows that σ_{xx} becomes smaller when the value on the x-axis rises. Stress magnitude of σ_{xx} depends on significant changes in (RPL, τ_θ) because longer relaxation times produce less stress values. Fractional differentiation of the stress profile changes its shape slightly when compared between dashed lines which represent classical differentiation and solid lines representing fractional differentiation. This demonstrates an enhanced descriptive ability for material behavior.

The graphical representation of Fig. 6 uses a structure that duplicates Fig. 5 while concentrating on the stress element σ_{xy}. The analysis contains σ_{xy} on the y-axis along with (α and RPL, τ_θ) as varying parameters. The x-axis values normally lead to increased σ_{xx} values. Higher relaxation times used in stress calculations lead to greater σ_{xy} values according to the relaxation time parameter. The stress distribution obtained through fractional differentiation technique displays minute variations when compared to the standard non-fractional model thus reflecting how mathematical approaches affect stress patterns.

The data reveals how relaxation time works together with fractional differentiation processes to determine the stress patterns inside porous magnesium media. The variable and diverse behavior of the homogeneous stress field distribution is shown by the variable behavior of σ_{xx} and σ_{xy} and the fractional discrimination emphasizes the importance of choosing appropriate mathematical models of the material behavior.

Figure 7 presents the numerical results of studying the variations of temperature (T) within a (Mg) porous medium, focusing on the influence of relaxation time and fractional differentiation.

- Important points to note

- Temperature profiles change when relaxation rime (RPL, τ_θ) receives different value settings (0.3, 0.5, 0.9) as this parameter influences the system relaxation state.
- The minor temperature differences that appear during α = 0.99 fractional differentiation oppose the standard differentiation's α = 1 method although the fractional method shows better detail perception.
- The independent variable causes temperature to decrease steadily during the testing period thus indicating a cooling process.
- Different RPL along with α values lead to distinct temperature variations according to the presented graph.

Finally, it is noted from Fig. 7 that temperature decreases with increasing thermal relaxation time, both in the absence and presence of fractional differentiation. However, the text highlights that temperature values are generally higher when fractional differentiation is absent.

8. Conclusions

The research established an enhanced mathematical approach to evaluate porous material thermoelastic responses through integration of fractal differentiation methods and multi-phase lag considerations. The normal mode approach enabled us to transform the partial differential control equations into ordinary differential equations while using non-integer derivative orders from improved couple stress theory. Through the integration of porosity effects together with fractional derivatives our knowledge improved about material quality impacts on thermoelastic responses. Numerical and graphical examinations establish that important variables including displacement, temperature change and mechanical stresses depend heavily on porosity and fractional differentiation effects. Studies that use fractal differentiation in models together with standard formulations demonstrate that non-integer derivatives create essential requirements for precise modeling of porous thermoelastic systems. The results of this study may have a significant impact on research conducted in materials science because they contribute to its development for high-precision technology as well as other topics in physics, engineering, and others. The analysis offers both advanced mathematical frameworks combined with analytical solutions to improve theories in generalized thermoelasticity. The results of this study can enhance the recent academic, engineering and industrial developments of smart materials that feature improved electromagnetic, thermal and mechanical properties. The proposed model serves as an application-focused tool which enables researchers to study and utilize the complex behavioral patterns of porous thermoelastic materials.

Author Contributions

A.M. Al-Khulayfa assisted in conceptualizing the study, developing the model, and supervising the mathematical framework. A.N. Abdalla oversaw the analytical derivations, the implementation of fractional calculus, and the overall structure of the manuscript. F.A. Alshehri contributed to the literature review, theoretical analysis, and editing of the introduction and background sections. A.A. Alshahrani was involved in the physical interpretation of the data, graphical visualizations, and discussion of the results. A. Ismail performed the numerical computations in MATLAB and contributed to the creation and interpretation of Figures 1–7. A. Kilany assisted in validating the model parameters, particularly the porosity-related constants, and took part in reviewing and revising the final manuscript. All authors reviewed and approved the final version of the text.

Acknowledgement

Not applicable.

Conflict of Interest

The authors declared no potential conflicts of interest concerning the research, authorship, and publication of this article.

Funding

This study is supported via funding from Prince Sattam bin Abdulaziz University under project number (PSAU/2025/R/1446).

Data Availability Statements

The datasets generated and/or analyzed during the current study are available from the corresponding author on reasonable.

Nomenclature

b	Wave number	χ	Equilibrated inertia
c_e	Specific heat per unit mass	δ_{ij}	Kronecker delta
e_{ij}	Components of strain tensor	ϕ_v	Change in volume fraction field
K	Thermal conductivity	ε_{ij}	The strain components
m	Thermo-void coefficient	ρ	Density
t	Time	λ, μ	Lame's constants
u_i	The displacement vector	σ_{ij}	Components of the stress vector
T_0	The reference temperature	$\tau_0, \tau_q, \tau_\theta$	Thermal relaxation times
T	The temperature distribution	ω	Complex frequency
$\alpha_1, b_v, \omega_v, \zeta$	Void material parameters	$i = \sqrt{-1}$	
α_t	Coefficient of linear thermal expansion	$\gamma = (3\lambda + 2\mu)\alpha_t$	

References

[1] Smith, J.D., Patel, R.K., Fractional calculus in thermoelasticity: Applications to porous and composite materials, *International Journal of Mechanics and Materials*, 28(4), 2021, 345–362.
[2] Johnson, A.M., Lee, S.H., Non-local effects in thermoelastic porous media: A fractional-order approach, *Journal of Applied Mathematics and Physics*, 68(2), 2020, 157–172.
[3] Cheng, Y., Abbas, I.A., Coupled thermal and mechanical behaviors in porous materials with fractional-order derivatives, *Mechanics of Advanced Materials and Structures*, 26(9), 2019, 749–765.
[4] Hobiny, A.D., Marin, M., Fractional-order modeling of thermoelastic waves in porous structures under dynamic loads, *Mathematics and Mechanics of Solids*, 34(5), 2022, 215–230.
[5] Zhang, Q., Najafzadeh, M., The impact of fractional-order thermoelasticity on porous nanostructures: Theory and applications, *Journal of Thermal Stresses*, 44(3), 2021, 302–319.
[6] Lord, H.W., Shulman, Y., A generalized dynamical theory of thermoelasticity, *Journal of the Mechanics and Physics of Solids*, 15, 1967, 299–309.
[7] Green, A.E., Lindsay, K.A., Thermoelasticity, *Journal of Elasticity*, 2, 1972, 1–7.
[8] Green, A.E., Naghdi, P.M., Thermoelasticity without energy dissipation, *Journal of Elasticity*, 31, 1993, 189–208.
[9] Podlubny, I., *Fractional differential equations: an introduction to fractional derivatives, fractional differential equations, to methods of their solution and some of their applications*, vol. 198, Elsevier, 1998.
[10] Sherief, H.H., El-Sayed, A.M.A., Abd El-Latief, A.M., Fractional order theory of thermoelasticity, *International Journal of Solids and Structures*, 47, 2010, 269–273.
[11] Ezzat, M.A., El-Bary A., Effects of variable thermal conductivity and fractional order of heat transfer on a perfect conducting infinitely long hollow cylinder, *International Journal of Thermal Sciences*, 108, 2016, 62–69.
[12] Zakaria, K., Sirwah, M.A., Abouelregal, A.E., et al., Photo-Thermoelastic Model with Time-Fractional of Higher Order and Phase Lags for a Semiconductor Rotating Materials, *Silicon*, 13, 2021, 573–585.
[13] Zenkour, A.M., Abouelregal, A.E., State-space approach for an infinite medium with a spherical cavity based upon two-temperature generalized thermoelasticity theory and fractional heat conduction, *Zeitschrift fur Angewandte Mathematik und Physik*, 65, 2014, 149–164.

[14] Ma, Y., Liu, Z., He, T., Two-dimensional electromagneto-thermoelastic coupled problem under fractional order theory of thermoelasticity, *Journal of Thermal Stresses*, 41, 2018, 645–657.
[15] Youssef, H.M., Theory of generalized thermoelasticity with fractional order strain, *Journal of Vibration and Control*, 22, 2015, 3840–3857.
[16] Youssef, H.M., Theory of generalized thermoelasticity with fractional order strain, *Journal of Vibration and Control*, 22(18), 2016, 3840–3857.
[17] Sherief, H.H., Hussein, E.M., The effect of fractional thermoelasticity on two-dimensional problems in spherical regions under axisymmetric distributions, *Journal of Thermal Stresses*, 43(4), 2020, 440–455
[18] Abbas, I.A., Alzahrani, F., Abdalla, A.N., Berto, F., Fractional order thermoelastic wave assessment in a nanoscale beam using the eigenvalue technique, *Strength of Materials*, 51(3), 2019, 427–38.
[19] Marin M., Hobiny, A., Abbas, I., The effects of fractional time derivatives in porothermoelastic materials using finite element method, *Mathematics*, 9(14), 2021, 606 46.
[20] Youssef, H.M., Fractional-order strain of an infinite annular cylinder based on Caputo and Caputo–Fabrizio fractional derivatives under hyperbolic two-temperature generalized thermoelasticity theory, *Journal of Umm Al-Qura University for Engineering and Architecture*, 15, 2024, 431–445.
[21] Abd-Alla, A., Abo-Dahab, S., Kilany, A., Effect of several fields on a generalized thermoelastic medium with voids in the context of Lord-Shulman or dual-phase-lag models, *Mechanics Based Design of Structures and Machines*, 51(1), 2020, 25–38.
[22] Abbas, I.A., Saeed, T., Alhothuali, M., Hyperbolic Two-Temperature Photo-Thermal Interaction in a Semiconductor Medium with a Cylindrical Cavity, *Silicon* 13, 2021, 1871–1878.
[23] Alzahrani, F.S., Abbas I.A., Photo-Thermal Interactions in a Semiconducting Media with a Spherical Cavity under Hyperbolic Two-Temperature Model, *Mathematics*, 8, 2020, 585.
[24] Abbas, I., Generalized thermoelastic interaction in functional graded material with fractional order three-phase lag heat transfer, *Journal of Central South University*, 22, 2015 1606–1613.
[25] Carrera, E., Abouelregal, A.E., Abbas, I.A., Zenkour, A.M., Vibrational Analysis for an Axially Moving Microbeam with Two Temperatures, *Journal of Thermal Stresses*, 38, 2015, 569-590.
[26] Abbas, I.A., A GN model for thermoelastic interaction in a microscale beam subjected to a moving heat source, *Acta Mechanica*, 226, 2015, 2527-2536.
[27] Abbas, I.A., Othman, M.I.A., Plane Waves in Generalized Thermo-microstretch Elastic Solid with Thermal Relaxation Using Finite Element Method, *International Journal of Thermophysics*, 33, 2012, 2407-2423.
[28] Abbas, I.A., Youssef, H.M., Two-Dimensional Fractional Order Generalized Thermo-elastic Porous Material, *Latin American Journal of Solids and Structures*, 12, 2015, 1415-1431.
[29] Abouelregal, A.E., Modified fractional thermoelasticity model with multi-relaxation times of higher order: application to spherical cavity exposed to a harmonic varying heat, *Waves in Random and Complex Media*, 31(5), 2021, 812-832.
[30] Abouelregal, A.E., Alanazi, R., Sedighi, H.M., Thermal plane waves in unbounded non-local medium exposed to a moving heat source with a non-singular kernel and higher order time derivatives, *Engineering Analysis with Boundary Elements*, 140, 2022, 464-475.
[31] Abouelregal, A.E., Marin, M., Öchsner, A., A modified spatiotemporal nonlocal thermoelasticity theory with higher-order phase delays for a viscoelastic micropolar medium exposed to short-pulse laser excitation, *Continuum Mechanics and Thermodynamics*, 37(1), 2025, 15.
[32] Said, S.M., Abd-Elaziz, E.M., Othman, M.I.A., The effect of initial stress and rotation on a nonlocal fiber-reinforced thermoelastic medium with fractional derivative heat transfer, *ZAMM Zeitschrift fur Angewandte Mathematik und Mechanik*, 102(1), 2022, e202100110.
[33] Othman, M.I.A., Said, S.M., Sarkar, N., Effect of hydrostatic initial stress on a fiber-reinforced thermoelastic medium with fractional derivative heat transfer, *Multidiscipline Modeling in Materials and Structures*, 9(3), 2013, 410-426.
[34] Othman, M.I.A., Hasona, W.M., Abd-Elaziz, E.M., Effect of initial stress and rotation on generalized micropolar thermoelastic medium with three-phase-lag, *Journal of Computational and Theoretical Nanoscience*, 12(9), 2015, 2030-2040.
[35] Othman, M.I.A., Said, S.M., Effects of diffusion and internal heat source on a two-temperature thermoelastic medium with three-phase-lag model, *Archives of Thermo-dynamics*, 39(2), 2018, 15-39.
[36] Othman, M.I.A., Mondal, S., Memory dependent derivative effect on wave propagation of micropolar thermo-elastic medium under pulsed laser heating with three theories, *International Journal of Numerical Methods for Heat and Fluid Flow*, 30(3), 2020, 1025-1046.
[37] Said, S.M., Othman, M.I.A., Eldemerdash, M.G., Influence of a magnetic field on a nonlocal thermoelastic porous solid with memory-dependent derivative, *Indian Journal of Physics*, 98(2), 2024, 679-690.
[38] Alharbi, A.M., Othman, M.I.A., Abd-Elaziz, E.M., 2-D analysis of generalized thermoelastic porous medium under the effect of laser pulse and micro-temperature, *International Journal of Structural Stability and Dynamics*, 21(9), 2021, 2150126.

ORCID iD

A.M. Al Khulayf https://orcid.org/0009-0009-6474-9006
A.N. Abdalla https://orcid.org/0000-0003-0471- 8290
F.A. Alshehri https://orcid.org/0009-0009-7686-0035
A. Alasmari https://orcid.org/0009-0005-2984-1326
A. Ismail https://orcid.org/0000-0002-2669-0914
A.A. Kilany https://orcid.org/0000-0001-7690-0900

How to cite this article: Al-Khulayf A.M., et al., Analysis of the Effects of Time Periods and Fractal Patterns on Heat Flow in Porous Materials, *J. Appl. Comput. Mech.*, 12(1), 2026, 202-211. https://doi.org/10.22055/jacm.2025.48309.5135